UNIVERSITY OF CALIFORNIA, SAN DIEGO
SCRIPPS INSTITUTION OF OCEANOGRAPHY
VISIBILITY LABORATORY
SAN DIEGO, CALIFORNIA 92152

VISUAL ASPECTS OF AIR COLLISION AVOIDANCE: COMPUTER STUDIES ON PILOT WARNING INDICATOR SPECIFICATIONS

Gerald D. Edwards and James L. Harris, Sr.

SIO Ref. 72-3
February 1972

Final Report

NASA-Ames Research Center
Grant No. NGR-05-009-059

Approved:

Seibert Q. Duntley, Director
Visibility Laboratory

Approved for Distribution

William A. Nierenberg, Director
Scripps Institution of Oceanography

ABSTRACT

This report describes techniques of computer calculations used to analyze the potential for improving visual acquisition of collision threats by means of Pilot Warning Indicator systems (PWI). It is a parametric study giving the quantitative effects of PWI resolution and effective range upon the average cumulative probability of detection.

VISUAL ASPECTS OF AIR COLLISION AVOIDANCE :

COMPUTER STUDIES ON PILOT WARNING INDICATOR SPECIFICATIONS

1. INTRODUCTION

Aircraft collisions are a problem of concern to both the aviation industry and the general public. Heavier air traffic and widespread awareness through mass communication are acting to intensify that concern.

Many solutions have been proposed to eliminate the occurrence of midair collisions. Some solutions are based upon changes and additions to government-enforced aviation rules and procedures. Others are dependent upon modifications and extensions of the Federal Aviation Administration's air traffic control program. Still other approaches call upon new sophisticated electronic systems which have the ability to exert positive control over all air traffic. Perhaps the long term solution is any one or any combination of these. In any event, current federal regulations place the responsibility for collision avoidance with the flight crew, whose visual performance plays a key role in the threat situation.

Consider, for instance, the case where one or both given aircraft are flying under Visual Flight Rules. Here the ability to detect and recognize an air collision threat depends heavily on the human visual system. But in a significant number of air collisions, successful evasive action did not occur because sighting of the threat craft was not made soon enough, at sufficient range.

In an effort to strengthen the visual performance of pilots and aircrews, considerable technical attention has been given to a class of supplementary instruments known as pilot warning indicators (PWI). These PWI devices are intended to alert the flight deck members that another aircraft is within range to pose an air collision threat. At that time the flightcrew would devote every effort to make a visual detection of the threat, analyze the situation and take appropriate action quickly.

Under previous funding from NASA-Ames Research Center, the Visibility Laboratory has developed techniques of computer calculation which allow quantitative evaluation of the probability of visual acquisition of an aircraft posing a collision threat. This report describes the use of those techniques in analyzing the potential for improving visual acquisition by means of PWI systems.

2. VISUAL CAPABILITIES AND LIMITATIONS

The probability of visual detection of an aircraft is dependent on many variables The aircraft has a complex three-dimensional shape and reflectance properties are associated with each of its surfaces The aircraft is illuminated by sky, sun, and terrain. Viewed from any path of sight the aircraft has a pattern of luminance values. The background against which the aircraft is viewed, either sky or terrain, determines the contrast pattern which will be seen. The atmosphere serves to reduce the contrast of the aircraft as it will appear to the observer due primarily to the scattering of image-forming light from the aircraft out of the path of sight and scattering of sky, sun, and terrain light into the path of sight. The ability of the human observer to detect the received visual stimulus is dependent upon fundamental thresholds of the eye These thresholds differ dramatically depending upon the retinal location of the aircraft image, i.e., where the eye is fixated relative to the location of the aircraft. A later section of this report describes the manner in which these factors are taken into account in a Visibility Engineering calculation.

Figure 1 shows a sample calculation designed to illustrate the role of PWI equipment. It is assumed that a Cessna 180 is closing head-on with a faster aircraft so that the closing velocity is 320 knots. The right-hand curve shows the cumulative probability of visual detection as a function of the time before impact, assuming that the observer devotes full time to visual acquisition and that he knows exactly where to look for the aircraft. Under these favorable conditions the observer reaches a probability of 1 at approximately 15 seconds before impact

Under many conditions, however, the observer does not know where the aircraft will be located within his field of view and cockpit duties preclude his devoting full time to visual vigilance One study has indicated that aircrews spent approximately 20 percent of their time in visual search.[1]

In that an air carrier pilot is concerned mainly with possible proximity to a slower general aviation aircraft, he might reasonably confine his normal search to a ±30 degree horizontal field and a ±7.5 degree vertical field. Assuming this search area as well as the 20 percent time devoted to visual search, the calculations produce the results shown by the left-hand curve in Fig 1 Here we see only a 14 probability of detection at 10 seconds before impact

These two extreme curves in Fig. 1 illustrate the potential for a PWI system. If the left-hand curve represents normal operating procedure, then the function of a PWI system is to (1) alert the pilot to a possible collision situation, thus causing him to devote more time to visual search and (2) give some indication to the pilot of the location of the threat, thus reducing the required search sector In this sense, the right-hand curve represents the performance achievable with the best possible PWI system, i.e., one which causes the pilot to devote full time to search and tells the pilot exactly where the threat is located.

Translating these two PWI functions into engineering terminology, they become detection range and angular resolution. That the PWI resolution is an important parameter is illustrated by the middle curve in

[1]Harry W. Orlady, "Selected Visual Problems of an Airline Pilot," Proceedings of the Spring Meeting 1969 NAS-NRC Committee on Vision, Visual Factors in Transportation Systems, pp 56–70.

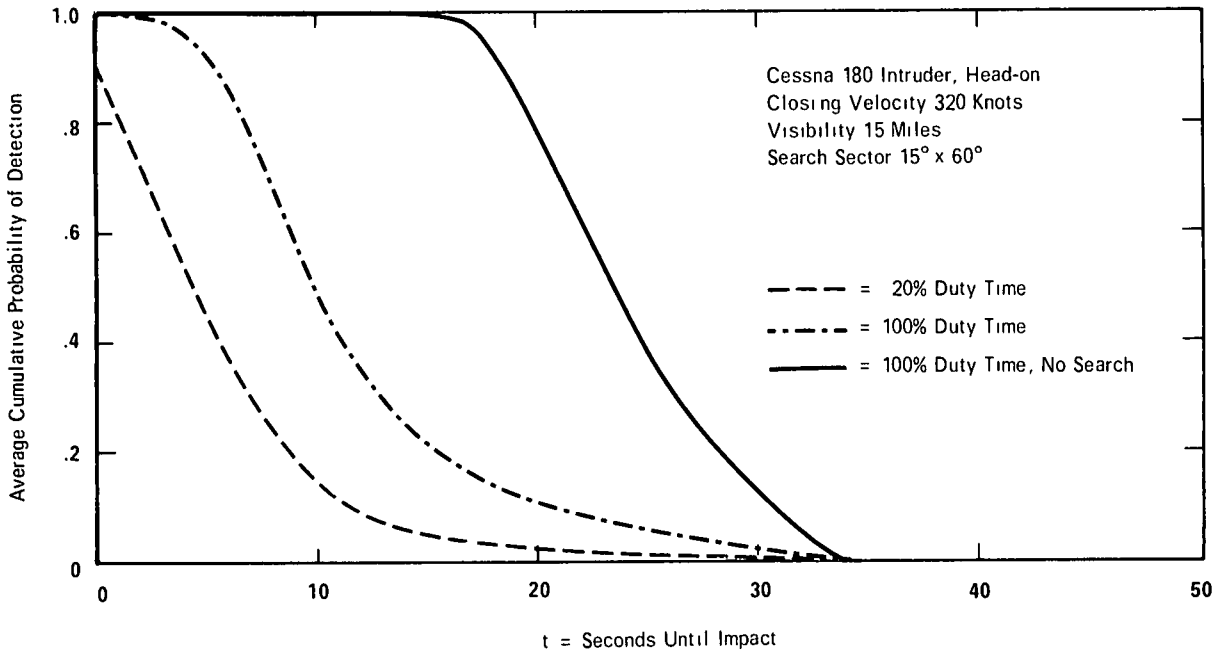

Figure 1. Average Cumulative Probability of Detection Versus Time Until Impact.

Fig. 1. Here the observer is warned of the presence of a threat but is given no information as to the location of the threat. He therefore devotes full time to search but must cover the entire 60 by 15 degree field. The curve shows that such a system would be limited to raising the detection probability from .14 to about .49 at 10 seconds before impact. Such a "warning-only" system falls far short of achieving the potential visual performance where location of the aircraft is also supplied.

Extreme caution should be exercised in drawing general conclusions from this illustrative example. It represents one aircraft type under one specific lighting geometry and for one specific closing geometry. Many such calculations should be made exploring the important parameters before generalizations as to the probability of visual acquisition can be properly made.

3. DEFINITION OF TASK

The basic objective of this study is to explore two very important engineering specifications of any PWI system: effective range and angular resolution. Effective range R_{max} is defined as the distance, between the observer and the intruder aircraft, at which the PWI gives the alarm. Angular resolution is defined as the azimuth search sector Az° within which the PWI system can locate an intruder aircraft.

4. COMPUTER PROCEDURES

The Visibility Laboratory computer installation, shown in Fig. 2 and 3, is an IBM System 360/44. The physical characteristics of the System 360/44 are listed below.

Unit	Description
2044	Central Processing Unit with 1 microsecond, 32K-32 bit word core and disk storage of 1×10^6 bytes
1442	Card Read-Punch, 400 cards/minute
1443	Line Printer, 240 lines/minute
2415	Magnetic Tape Unit, two drives, nine track, 15 000 bytes/second
2841	Disk Storage Control
2311	Disk Drive with 1316 cartridge, 7.5×10^6 bytes
2701	Data Adapter Unit
2741	Communication Terminal: One 16-bit analog to digital converter Two 16-bit contact operate banks Three 16-bit digital input groups Two 13-bit digital to analog converters

The image dissector scanner,[2] shown in Fig. 4, is a device for converting optical signals into electrical signals. It was used to electro-optically scan the selected models and transfer the resultant luminance map into the computer.

The software techniques employed in this study are directed toward calculating the average cumulative probability of detection. The average cumulative probability of detection is range-dependent and results from all visual fixations from the start of a search for a target somewhere within the prescribed search sector. Purely random search by the observer was assumed in this study.

Accurate scale model aircraft were illuminated and electro-optically scanned to generate inherent contrast maps. The illumination was for the case of a sun position of 30-degree elevation and 150-degree azimuth relative to the observer's line of sight. When any conclusions are drawn based upon calculations using these contrast maps as basic inputs, the above restrictions should be remembered. Vision research

[2]B. McGlamery, M. Myers, R. Ensminger and R. Howarth, "Progress in Image Processing Techniques and Equipment," SIO Ref. 69-28, November 1969, AD 698359.

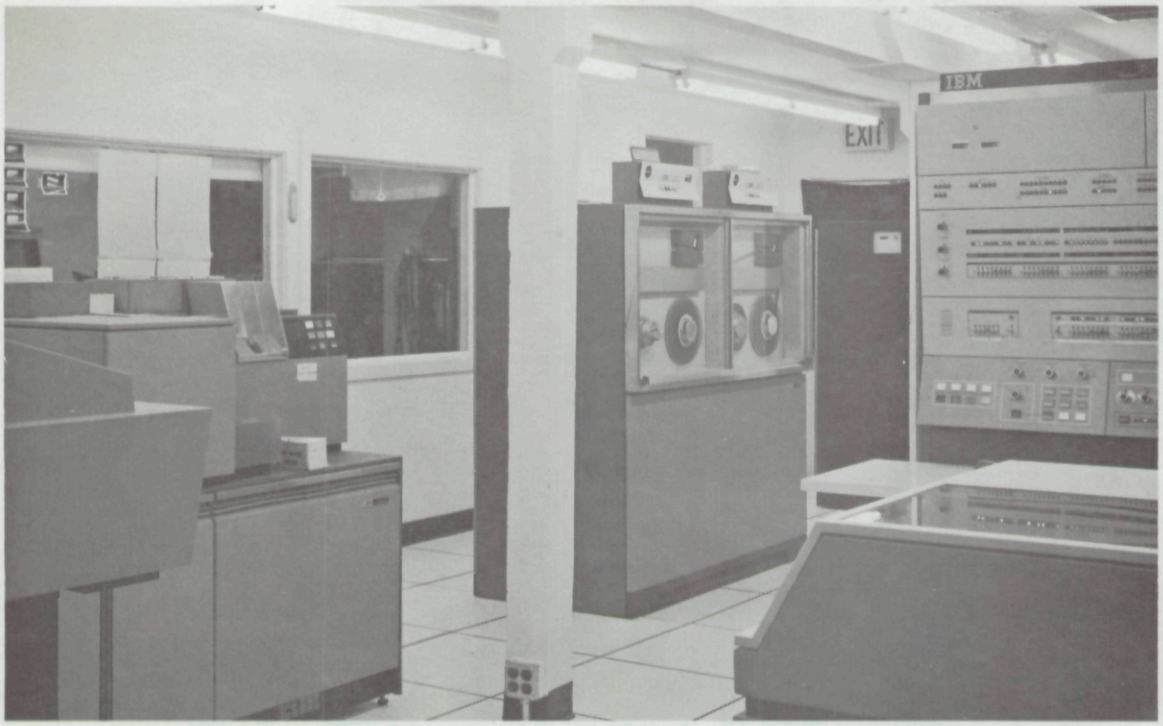

Figure 2. The IBM System 360/44 Computer.

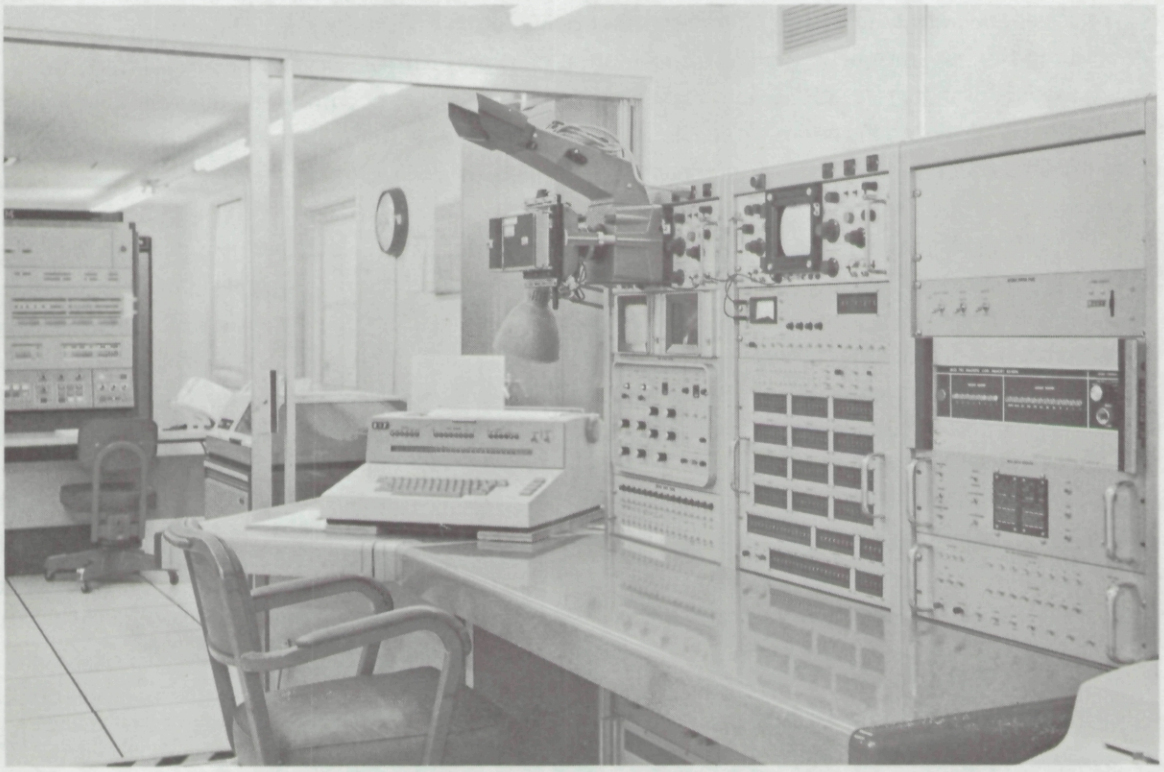

Figure 3. The IBM System 360/44 Computer and the Refresh Display Console.

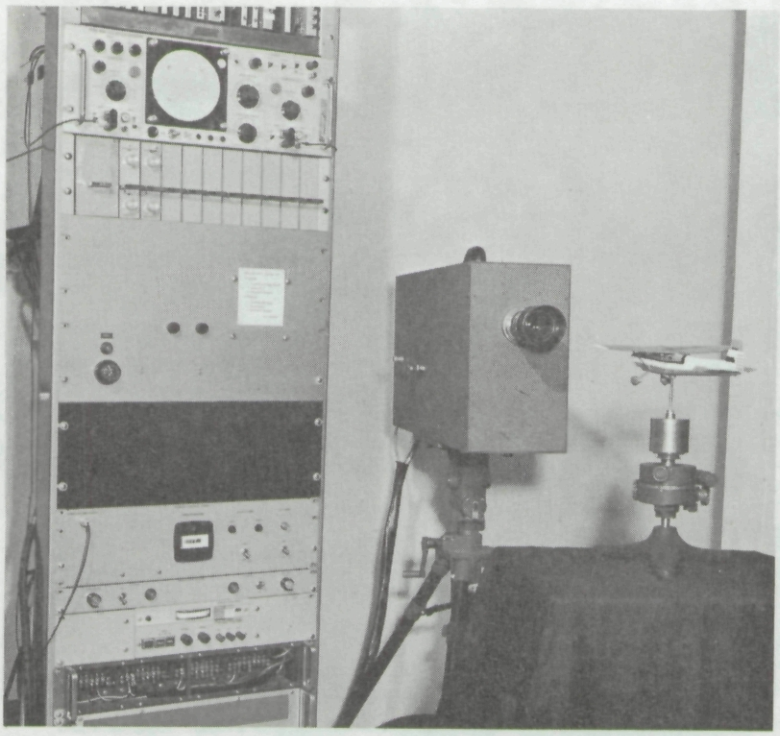

Figure 4. The Image Dissector Scanner.

data obtained by Dr. John Taylor of the Visibility Laboratory[3] were used to calculate a summative function for 1/3 of a second foveal fixation at an adaptation level of 75 foot-lamberts. Fourier techniques were used to convolve this visual threshold data and the aircraft contrast maps after both were scaled for range. Peak values were selected from the resultant convolution contrast maps. Figure 5 is a block diagram describing the generation of the peak convolution contrast $\hat{C}(R_i)$. Dr. Taylor's off-axis vision data were used to establish the relationship between the peak convolution contrast at the fovea and at other retinal locations. After application of atmospheric contrast attenuation, the retinal map of convolution contrasts allowed calculation of the retinal map of liminal threshold ratios.

The retinal map of liminal threshold ratios was then applied in evaluating the detection probability integral which gives us the single fixation probability of detection for every retinal point. Figure 6 is a block diagram describing the generation of the retinal map of single fixation detection probability. Again Fourier techniques were used to convolve this single fixation probability of detection map with the appropriate search sector. The result was a map of the average single fixation probability of detection. This average single fixation probability of detection at some point in the search sector is the average of all the values calculated for an aircraft located at that point with the visual axis fixated at every point in the search sector.

The cumulative probability of detection map for a finite range was calculated by multiplying the average probability of detection maps for all the fixations that occurred since the start of the visual search. The average value of the cumulative map was then plotted versus range as the average cumulative probability of detection. Figure 7 shows the block diagram of the generation of the average cumulative probability of detection $\bar{P}_c(R_i)$.

[3]John H. Taylor, "Contrast Thresholds as a Function of Retinal Position and Target Size for the Light-Adapted Eye," SIO Ref. 61-10, March 1961, AD 296243.

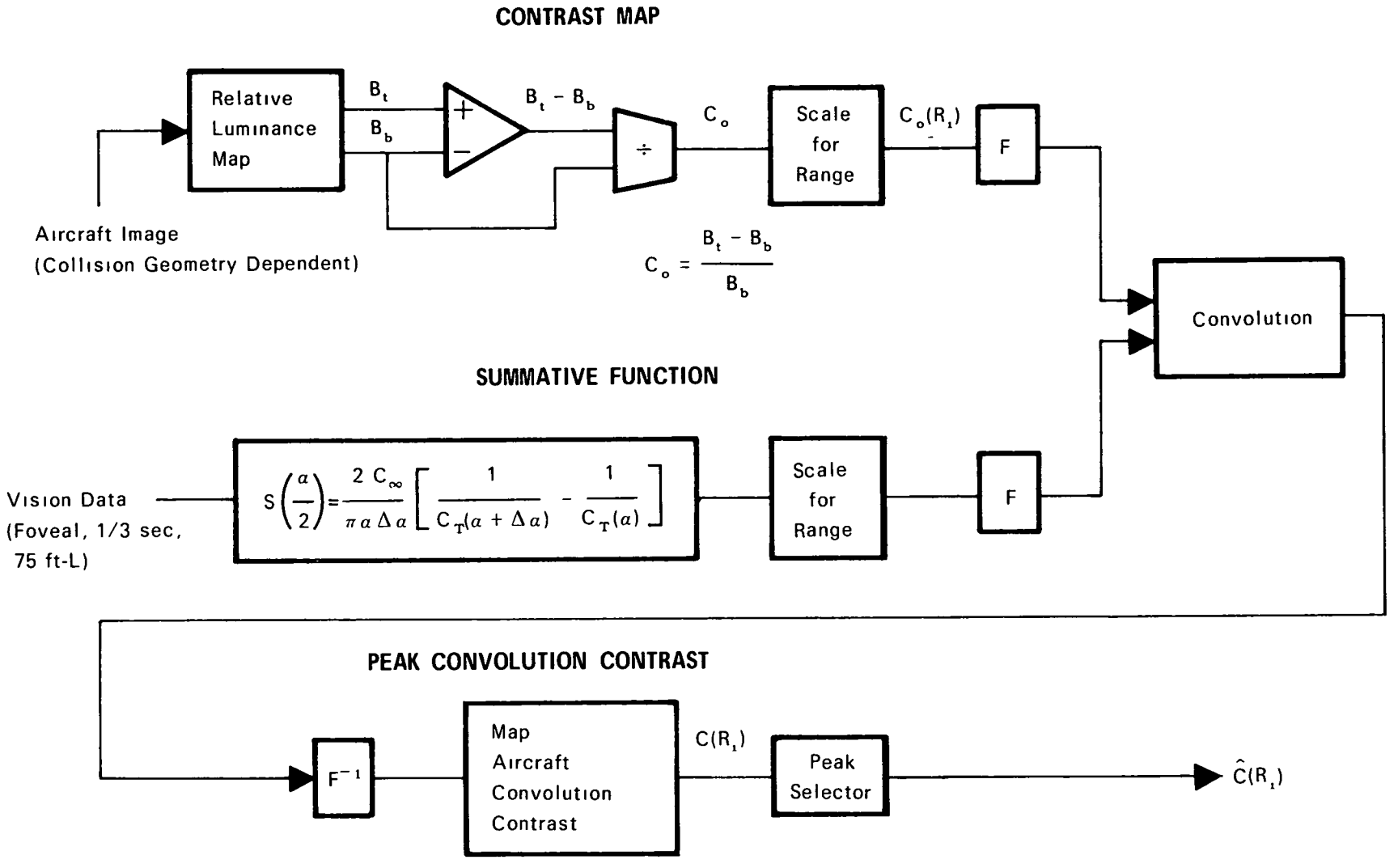

Figure 5. Block Diagram, Generation of Peak Convolution Contrast.

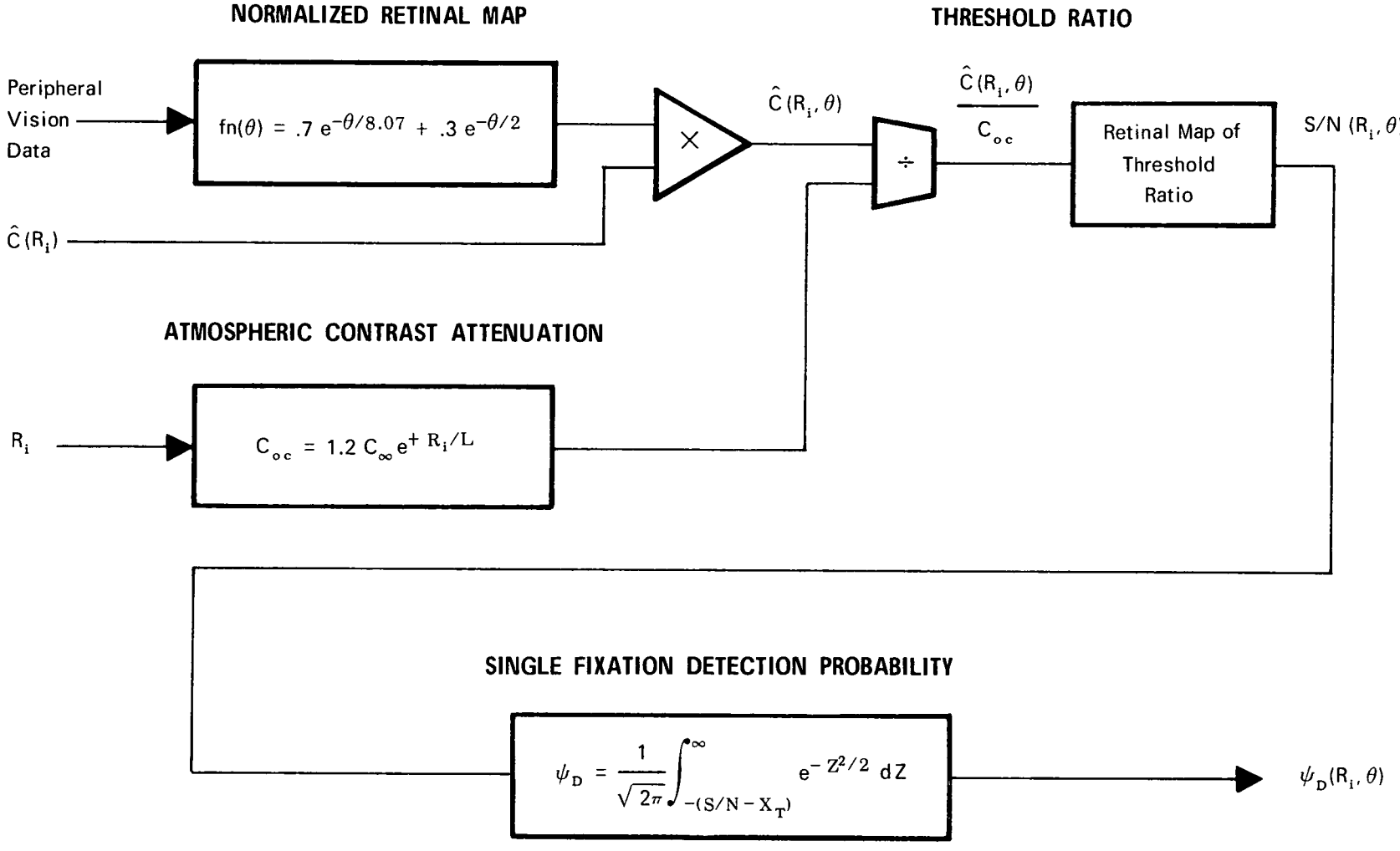

Figure 6. Block Diagram, Generation of Retinal Map of Single Fixation Detection Probability.

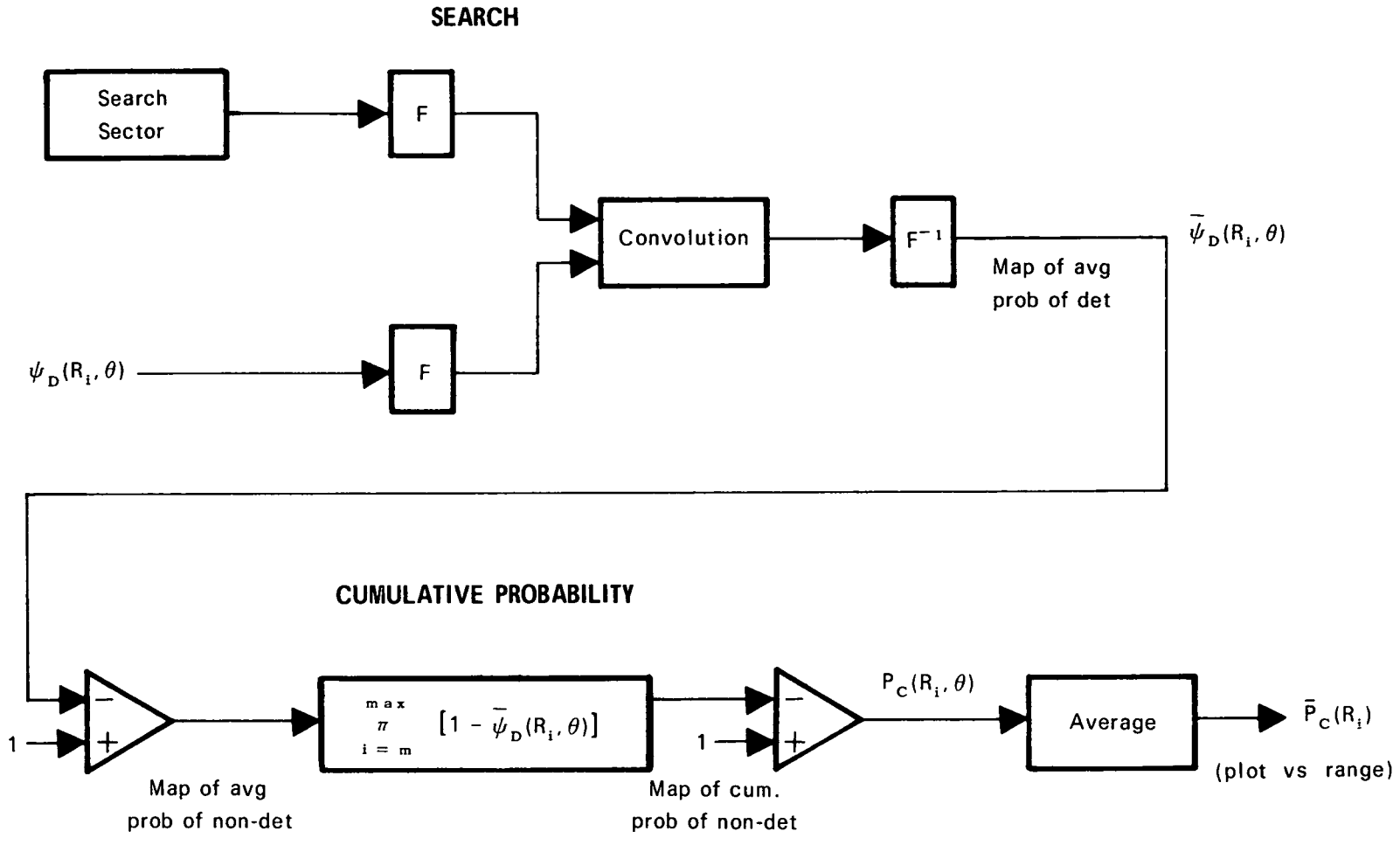

Figure 7. Block Diagram, Generation of $\bar{P}_c(R_i)$, Average Cumulative Probability of Detection.

COLLISION GEOMETRY

Any aircraft has a complex three-dimensional shape which creates a different cross-section and internal pattern from nearly every direction of view. In the classic collision course the relative bearings of the involved aircraft are fixed and the threatening aircraft presents a constant aspect at a fixed position in the observer's field of view. Aspect is the observer's angle of view of the intruder aircraft as measured from the intruder's flight direction. Figure 8 defines the collision geometry for this study. Table 1 gives the range R, the bearing β of the threatening aircraft, the closing angle γ as a function of the aspect σ, and the relative speed K of the observer's aircraft to that of the intruder's.

Two aircraft types were selected for study. A Cessna 180 represented the typical example of a general aviation aircraft used widely in the United States. A Douglas DC-8 was selected as the example of a commercial aircraft. See Fig. 9 and 10.

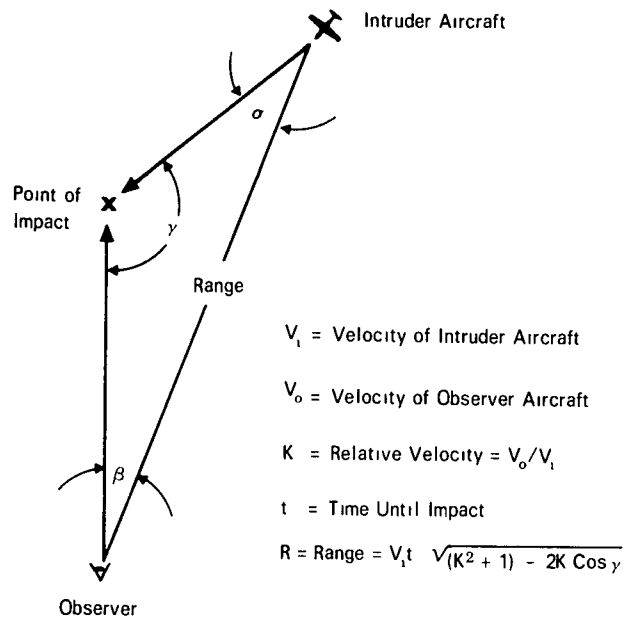

Figure 8. Collision Geometry.

Table 1. Collision Geometry

		σ (degrees)									
		0°	20°	40°	60°	80°	100°	120°	140°	160°	180°
K = 1	R	2 0$V_i t$	1 87$V_i t$	1 53$V_i t$	1 0 $V_i t$	35$V_i t$	-	-	-	-	-
	β	0°	20°	40°	60°	80°	-	-	-	-	-
	γ	180°	140°	100°	60°	20°	-	-	-	-	-
K = 2	R	3 0$V_i t$	2 91$V_i t$	2 65$V_i t$	2 31$V_i t$	1 92$V_i t$	1 57$V_i t$	1 32$V_i t$	1 13$V_i t$	1 03$V_i t$	1 0$V_i t$
	β	0°	10°	18 7°	25 3°	29 5°	29 5°	25 3°	18 7°	10°	0°
	γ	180°	150°	120 3°	94 7°	70 5°	50 5°	34 7°	21 3°	10°	0°
K = 3	R	4 0$V_i t$	3 92$V_i t$	3 70$V_i t$	3 37$V_i t$	3 01$V_i t$	2 63$V_i t$	2 38$V_i t$	2 16$V_i t$	2 04$V_i t$	2 0$V_i t$
	β	0°	6 5°	12 4°	16 7°	19 1°	19 1°	16 7°	12 4°	6 5°	0°
	γ	180°	153 5°	127 6°	103 3°	80 9°	60 9°	43 3°	27 6°	13 5°	0°
K = 4	R	5 0$V_i t$	4 92$V_i t$	4 71$V_i t$	4 40$V_i t$	4 05$V_i t$	3 70$V_i t$	3 42$V_i t$	3 18$V_i t$	3 04$V_i t$	3 0$V_i t$
	β	0°	5°	9 3°	12 5°	14 2°	14 2°	12 5°	9 3°	5°	0°
	γ	180°	155°	130 7°	107 5°	85 8°	65 8°	48 5°	30 7°	15°	0°

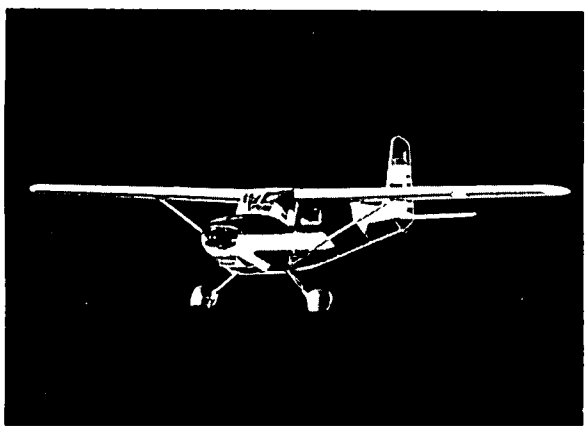

Figure 9. Scale Model of Cessna 180.

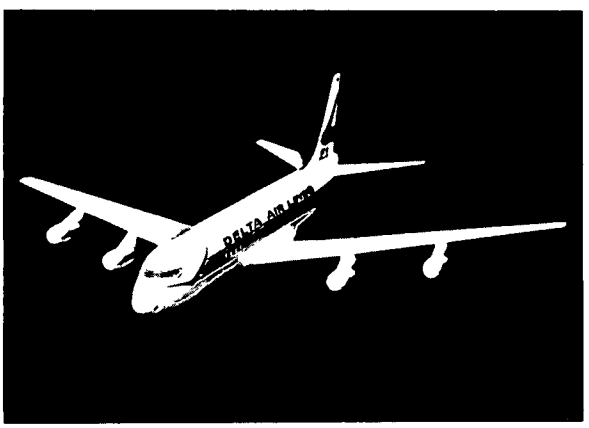

Figure 10. Scale Model of Douglas DC-8.

CALCULATIONS OF MAXIMUM VISUAL PERFORMANCE

The peak convolution contrast $\hat{C}(R_i)$ versus the aspect σ was calculated with the range as a constant. Figure 11 is the peak convolution contrast $\hat{C}(R_i)$ versus the aspect σ for the Cessna 180 and Fig. 12 is the peak convolution contrast $\hat{C}(R_i)$ versus the aspect σ for the DC-8. (Note the scale change on these two graphs.) An examination of Fig. 11 and 12 reveals the unsurprising fact that the peak convolution contrast is smallest where the cross-sectional area presented to the observer is minimum $\sigma = 0°$. Since minimum contrasts will give us minimum probabilities of detection, those aspects will be of prime interest to us.

The time until impact t is the time available to the observer for the entire process of alarm, visual search, detection and reaction. A comparison of plots of peak convolution contrast $\hat{C}(R_i)$ versus time until impact t will show which cases have the worst combinations of low contrast and minimum time intervals until impact.

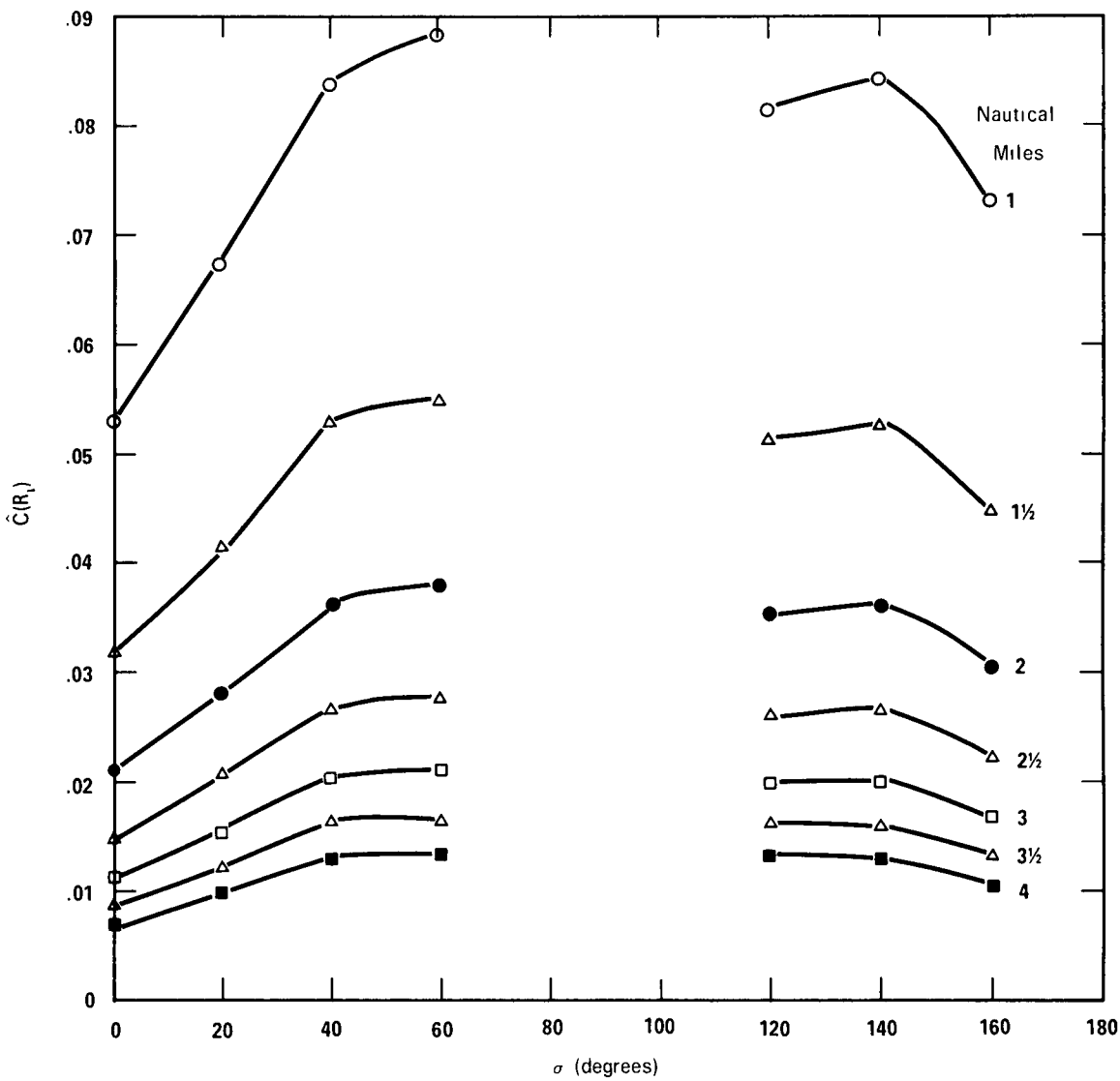

Figure 11. Peak Convolution Contrast Versus Aspect for Cessna 180.

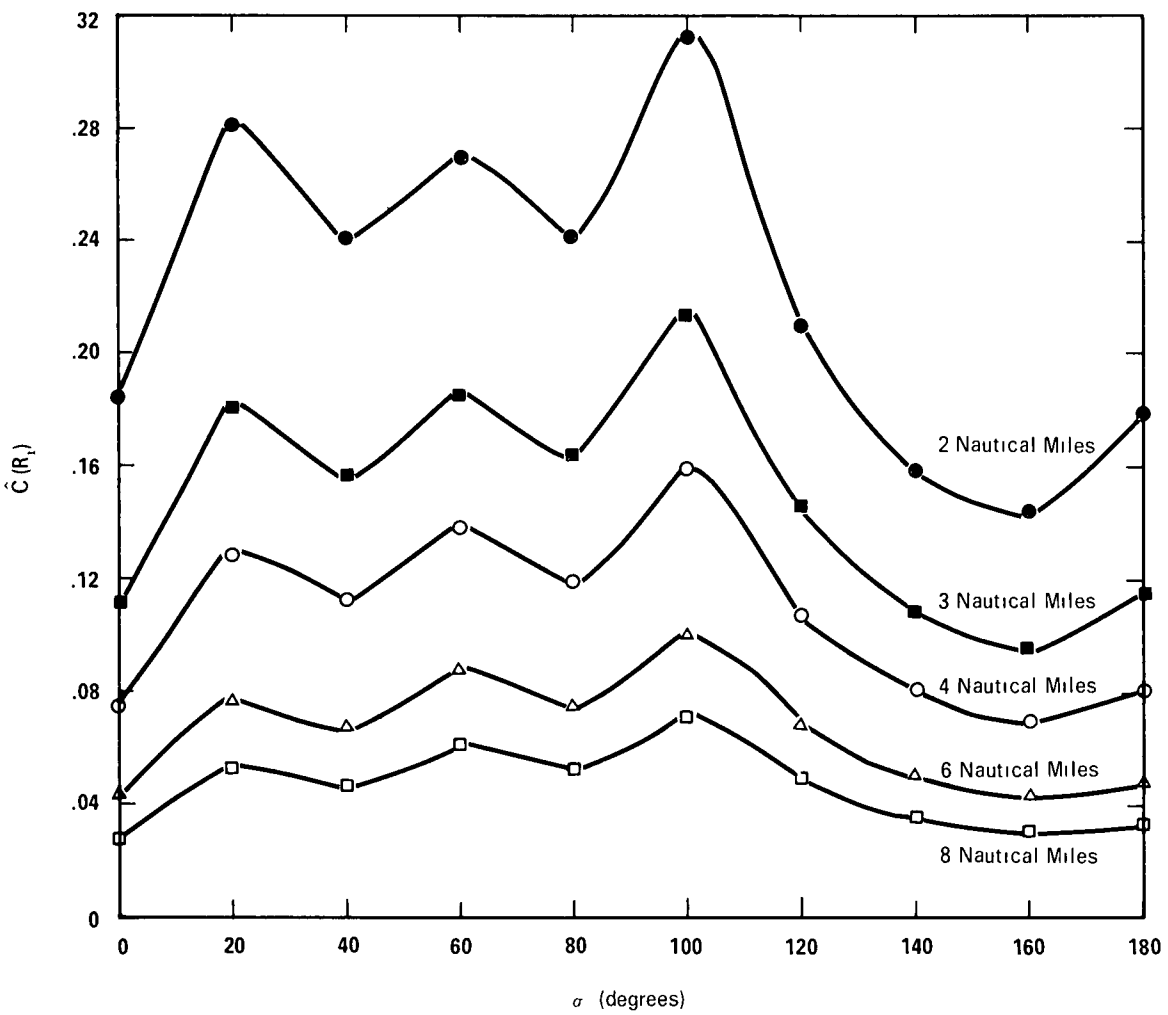

Figure 12. Peak Convolution Contrast Versus Aspect for DC-8.

Figure 13 shows peak convolution contrast $\hat{C}(R_i)$ versus time until impact t for a DC-8 as it approaches the observer head-on $\sigma = 0°$. In all cases the intruder aircraft (DC-8) has a velocity of 240 knots. The relative effect of the observer aircraft velocity is shown by the curves labeled K = 1/2, K = 1 and K = 2 which represent observer aircraft velocities of 120 knots, 240 knots and 480 knots, respectively.

Figure 14 shows the peak convolution contrast $\hat{C}(R_i)$ versus time until impact t for a Cessna 180 with the same collision geometry. The curves are drawn for an intruder aircraft velocity of 80 knots. The observer aircraft velocity ranges from 80 knots to 240 knots. Figures 13 and 14 are plotted on the same scale for ease of comparison. Such a comparison indicates that the Cessna 180 has a more critical combination of smaller contrasts and shorter time intervals until impact. Because the Cessna 180 configuration is more difficult to detect than the DC-8, the remainder of the study will deal exclusively with the case of the Cessna 180.

Let us examine further the Cessna 180 in this head-on geometry and with a relative speed of three. Does the human visual system have the inherent capability to detect a collision threat at a range sufficient to allow avoidance maneuver?

For this critical configuration the single fixation probability of detection ψ_D versus the seconds until impact is plotted in Fig. 15. The calculation assumes foveal fixation with no search requirement by the observer. In other words, it is the best an observer could do with a single 1/3 of a second fixation at that range if he knew precisely where the intruder aircraft would appear. Calculation of the cumulative probability of detection for this case would give the observer's performance for continual foveal fixations

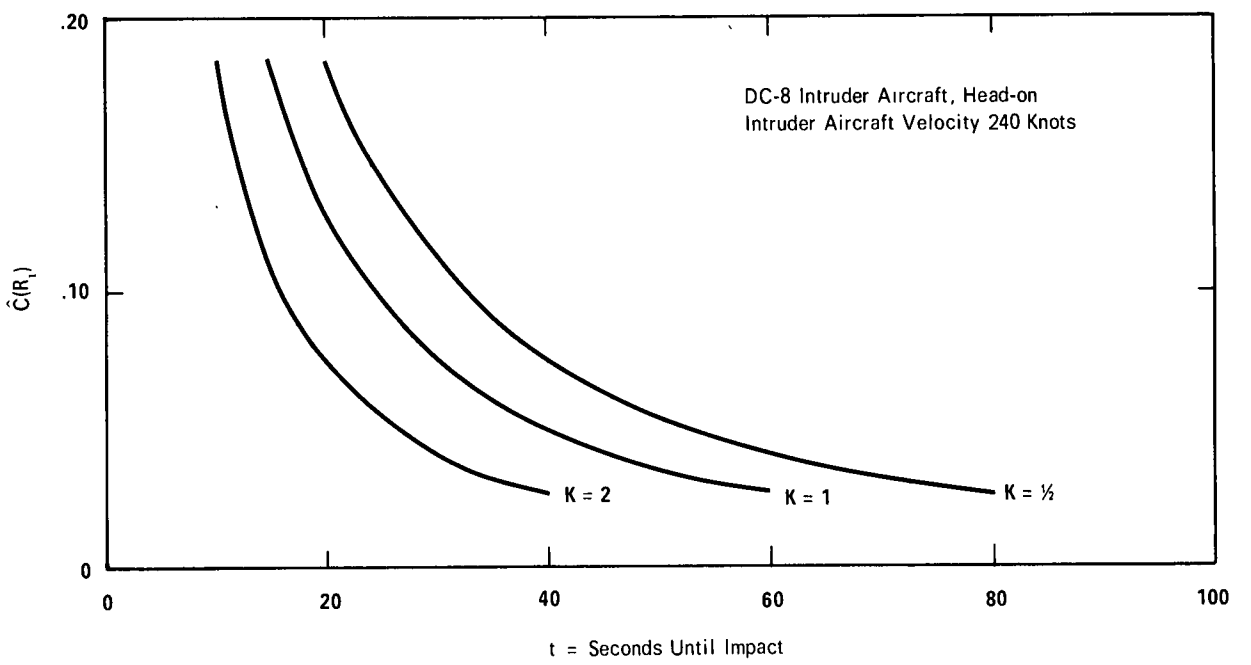

Figure 13. Peak Convolution Contrast Versus Time Until Impact for DC-8.

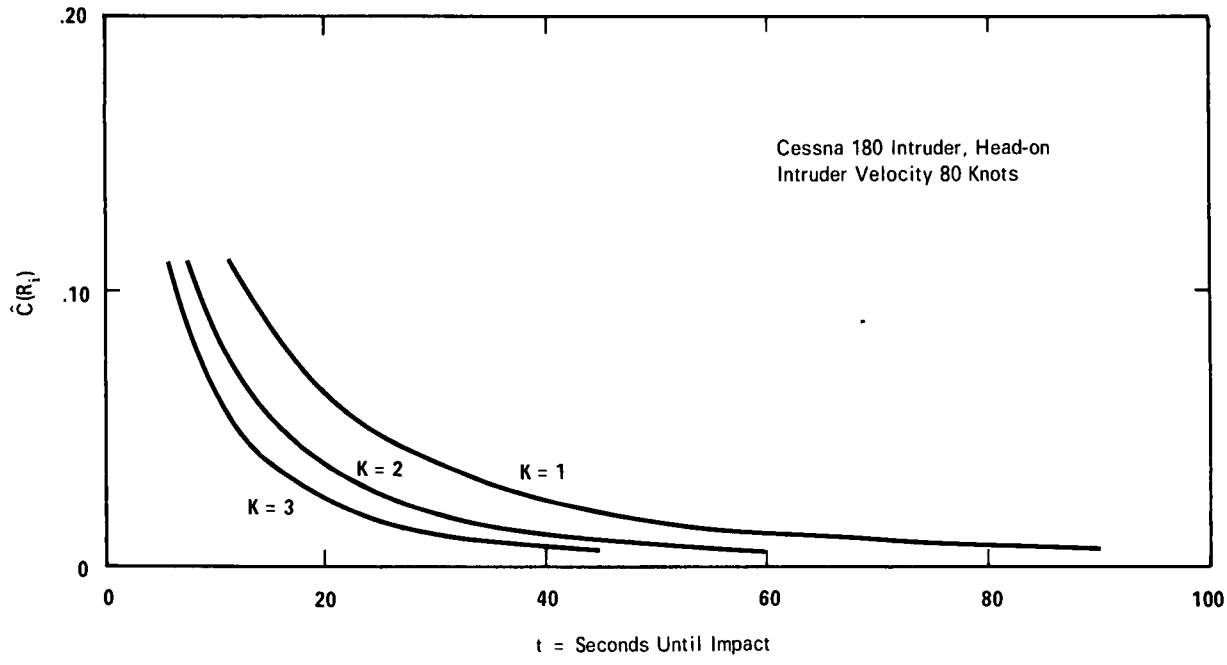

Figure 14. Peak Convolution Contrast Versus Time Until Impact for Cessna 180.

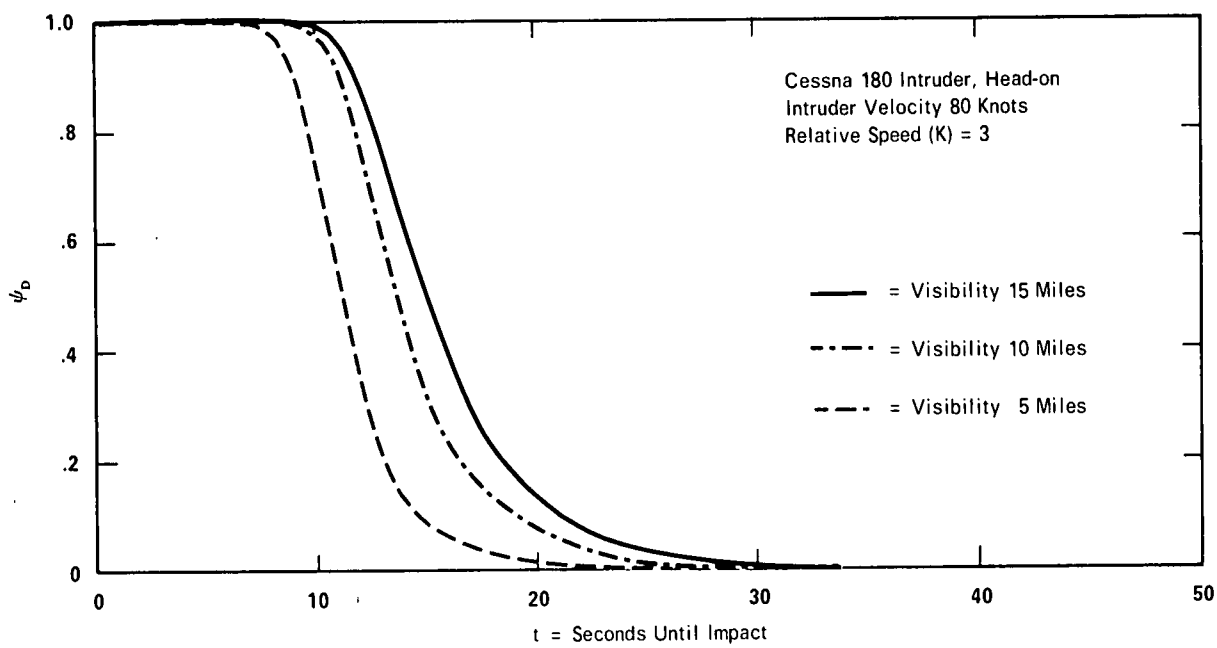

Figure 15. Single Fixation Probability of Detection Versus Time Until Impact for Cessna 180.

at the point in space where the intruder will appear. Figure 16 shows the cumulative probability of detection $P_c(R_1)$ versus the time until impact for the case where the visual fixations began at a range of 3 nautical miles.

Ten seconds has sometimes been stated as the minimum required time for visual acquisition if successful evasive action is to result. Examination of Fig. 16 shows that even with a visibility of only 5 miles, there is a .99 probability of detection at t = 11 seconds. Using this criterion and remembering that this case is for one particular aircraft, a particular adaptation level and a particular sun location, we can conclude that the human visual system does have the inherent detection capability to be effective in air collision avoidance.

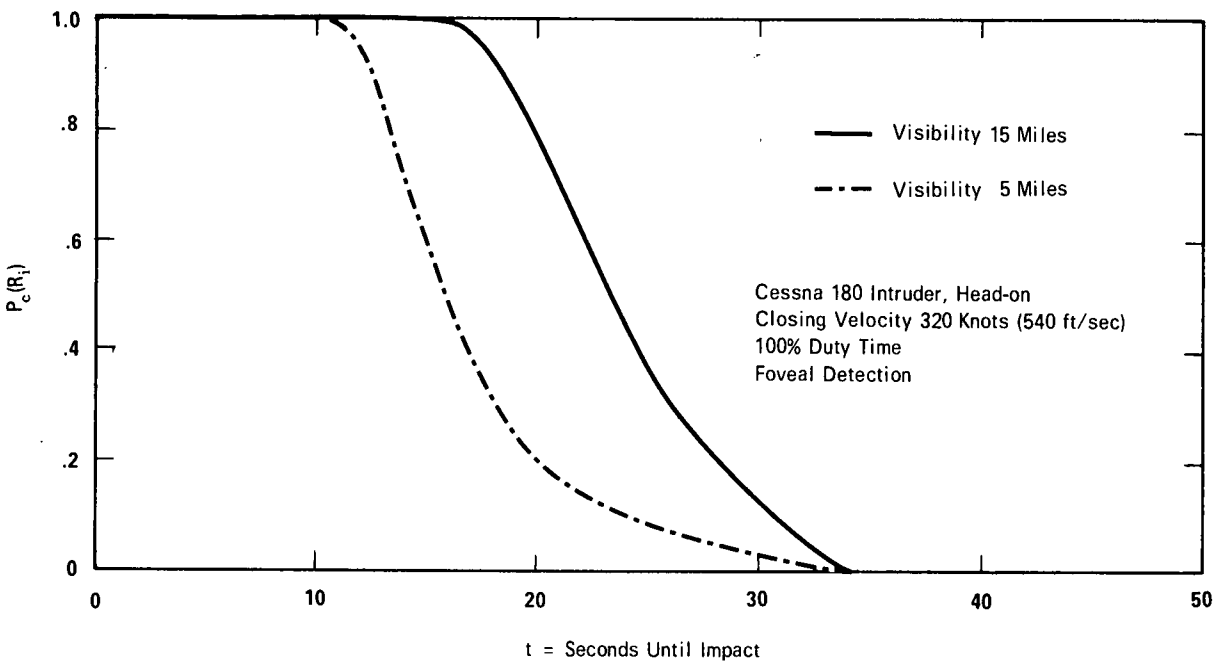

Figure 16. Cumulative Probability of Detection Versus Time Until Impact for Cessna 180.

5. PILOT WARNING INDICATOR SPECIFICATIONS

The calculations previously described indicate that the human visual system can be effective in air collision avoidance, if the observer has been alerted to the presence and location of the intruder aircraft. The PWI concept is proposed as the source for just such information.

Two specifications which affect the performance of the alerted observer are the effective range and the angular resolution with which the threat is defined to the pilot. The case of the Cessna 180 will be used to show the quantitative effect of the two parameters upon the average cumulative probability of detection.

EFFECTIVE RANGE

The effective range R_{max} of a PWI device is defined as the distance between observer aircraft and intruder aircraft at which the device sounds an alarm. The affect of this parameter upon the average cumulative probability of detection is shown in the following figures. All cases are for a Cessna 180 traveling at 80 knots.

Figure 17 – Average Cumulative Probability of Detection versus Time Until Impact, Cessna 180: bearing 0°, closing velocity 540 ft/sec, visibility 15 miles, aspect 0°, search sector 15° x 15°.

Figure 18 – Average Cumulative Probability of Detection versus Time Until Impact, Cessna 180: bearing 0°, closing velocity 540 ft/sec, visibility 15 miles, aspect 0°, search sector 15° x 30°.

Figure 19 – Average Cumulative Probability of Detection versus Time Until Impact, Cessna 180: bearing 0°, closing velocity 540 ft/sec, visibility 15 miles, aspect 0°, search sector 15° x 45°.

Figure 20 – Average Cumulative Probability of Detection versus Time Until Impact, Cessna 180: bearing 12.5°, closing velocity 498 ft/sec, visibility 15 miles, aspect 40°, search sector 15° x 30°.

Figure 21 – Average Cumulative Probability of Detection versus Time Until Impact, Cessna 180: bearing 6.5°, closing velocity 275 ft/sec, visibility 15 miles, aspect 160°, search sector 15° x 30°.

An examination of these figures shows the following two points. Bear in mind that the examination is based on an assumed criterion, i.e., 10 seconds is sufficient time in which to take evasive action.

(1) Significant increases in the average cumulative probability of detection where the effective range is increased from 1 to 2 nautical miles.

(2) Only nominal increase in the average cumulative probability of detection where the effective range is increased from 2 to 3 nautical miles. This is especially apparent in $\bar{P}_c$'s in excess of .50.

The improved results obtained by increasing the effective range R_{max} from 1 to 2 nautical miles would justify the 100 percent increase in time required for visual search. But the increased time for visual search realized by starting at 3 nautical miles shows little improvement in $\bar{P}_c(R_i)$. On this basis an effective range of 2 nautical miles is suggested.

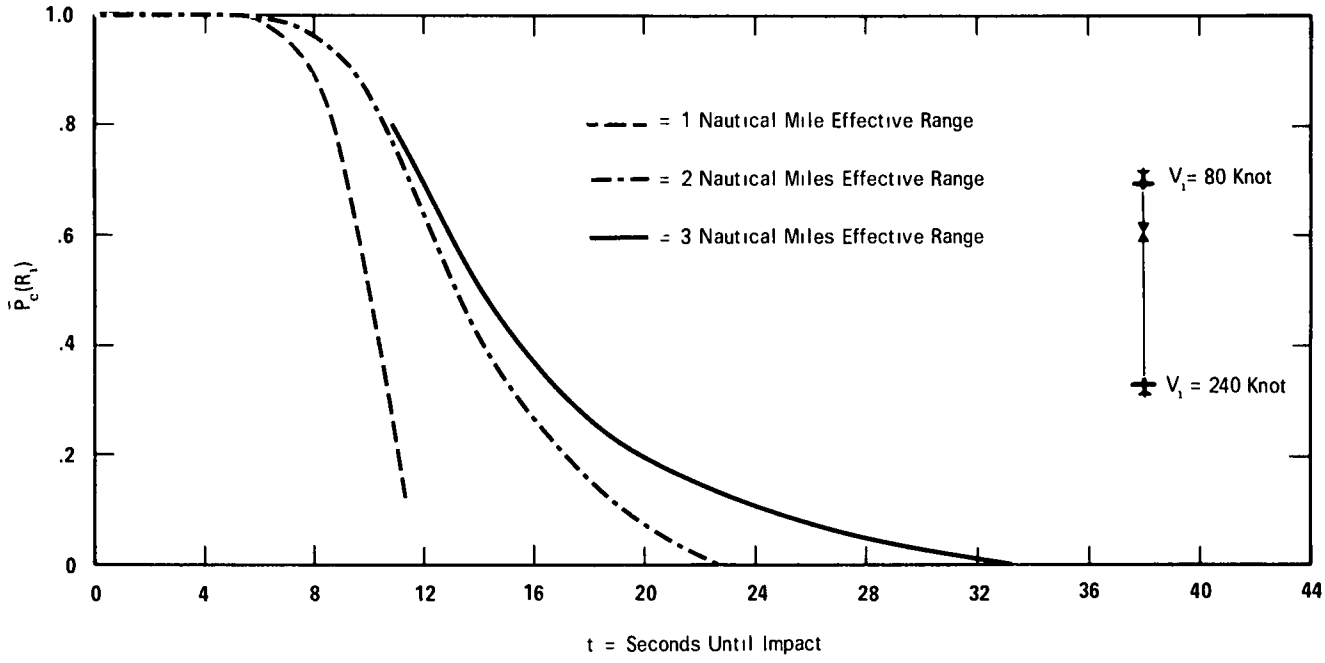

Figure 17. Average Cumulative Probability of Detection Versus Time Until Impact, Cessna 180· bearing 0°, closing velocity 540 ft/sec, visibility 15 miles, aspect 0°, search sector 15° x 15°.

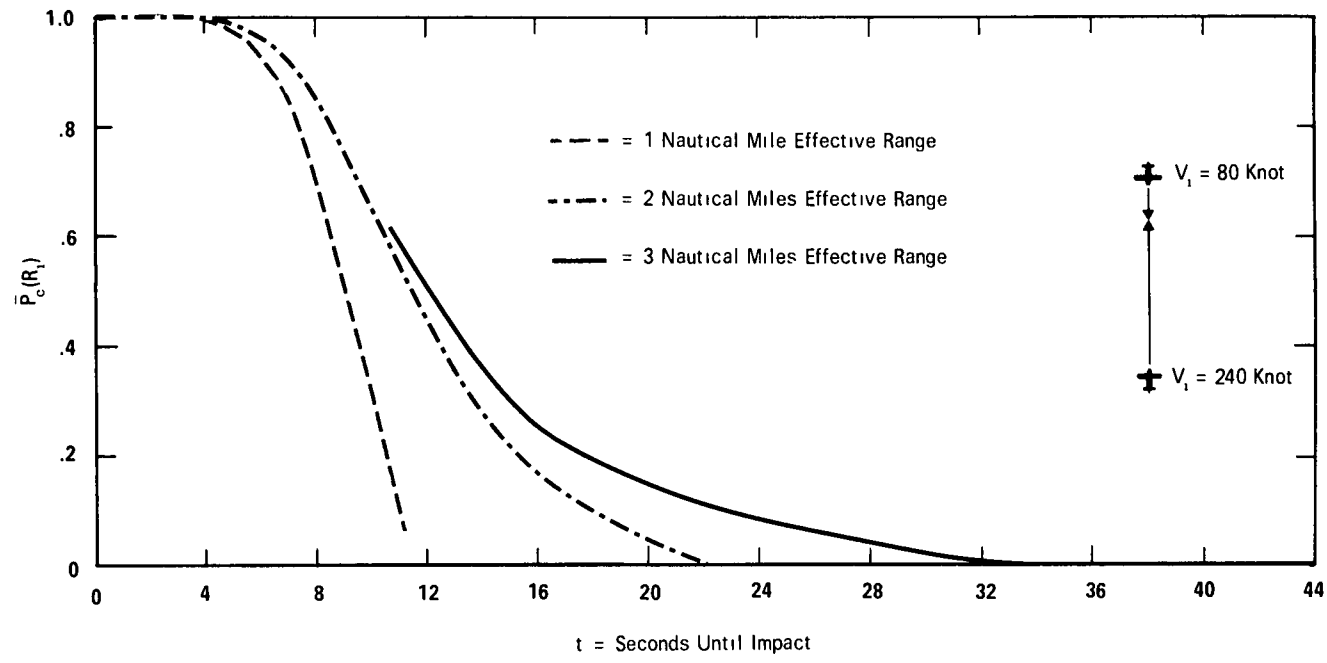

Figure 18. Average Cumulative Probability of Detection Versus Time Until Impact, Cessna 180 bearing 0°, closing velocity 540 ft/sec, visibility 15 miles, aspect 0°, search sector 15° x 30°.

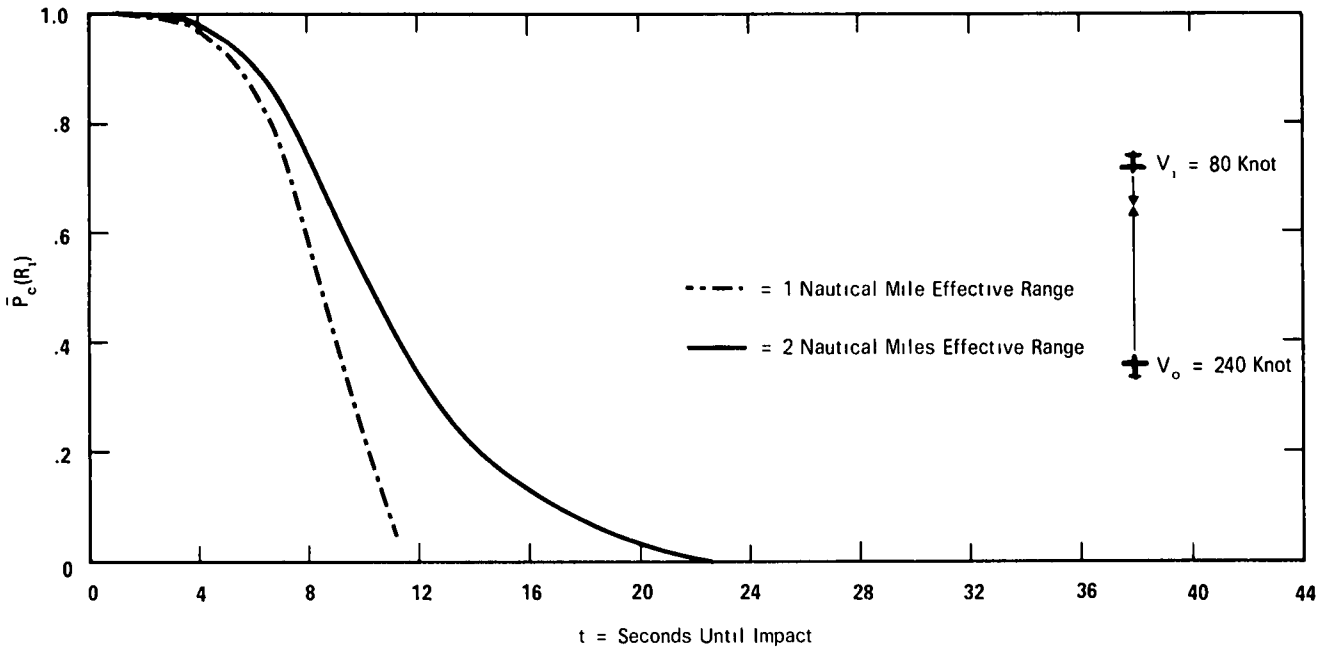

Figure 19. Average Cumulative Probability of Detection Versus Time Until Impact, Cessna 180 bearing 0°, closing velocity 540 ft/sec, visibility 15 miles, aspect 0°, search sector 15° x 45°.

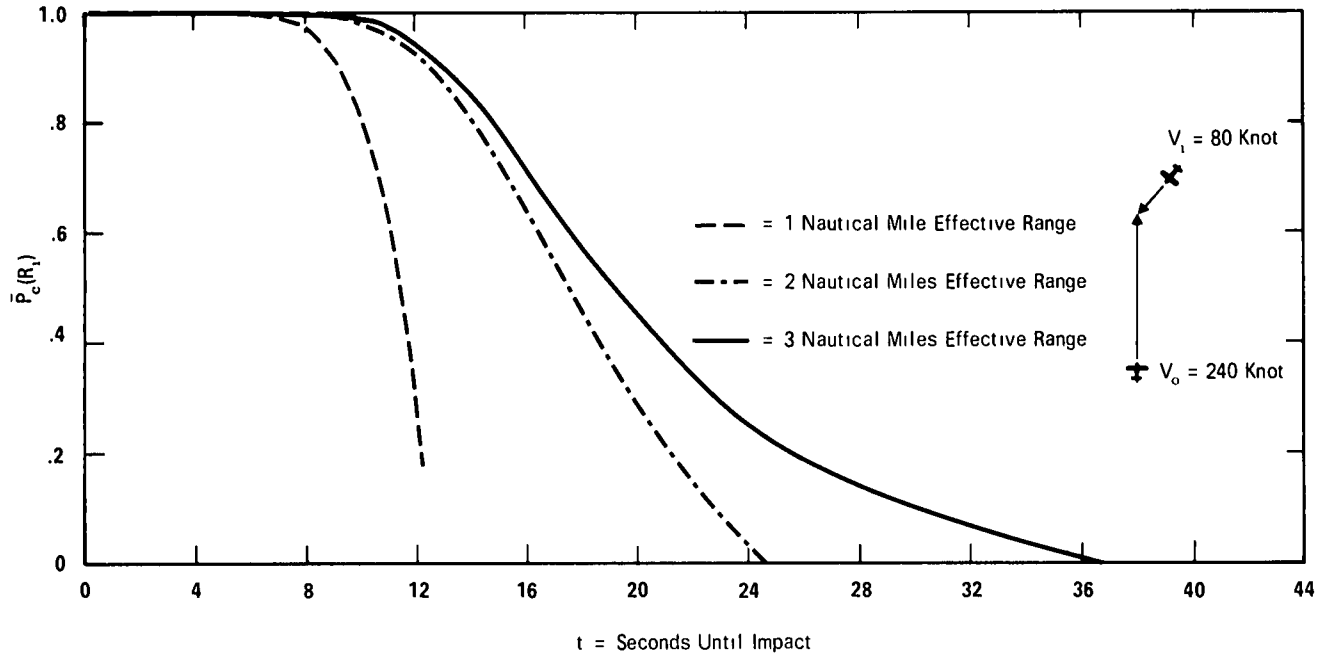

Figure 20. Average Cumulative Probability of Detection Versus Time Until Impact, Cessna 180 bearing 12.5°, closing velocity 498 ft/sec, visibility 15 miles, aspect 40°, search sector 15° x 30°.

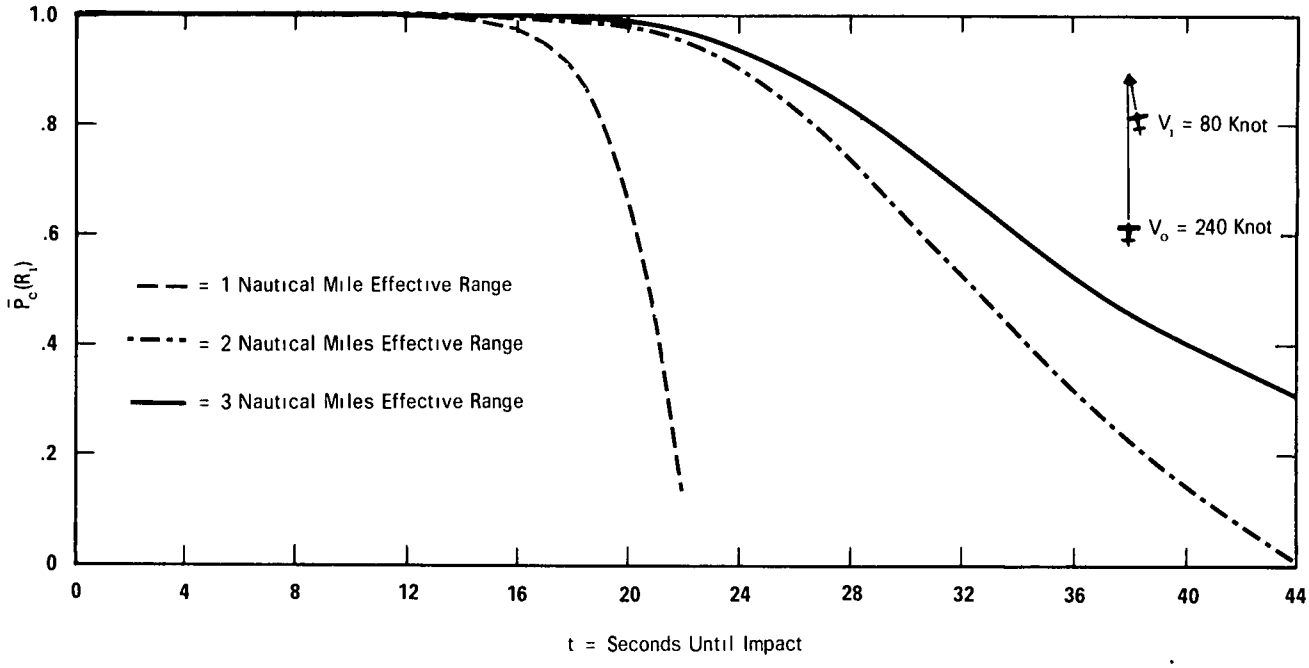

Figure 21. Average Cumulative Probability of Detection Versus Time Until Impact, Cessna 180: bearing 6.5°, closing velocity 275 ft/sec, visibility 15 miles, aspect 160°, search sector 15° x 30°.

SEARCH SECTOR

The search sector Az° used in this study is the azimuth arc of a rectangular visual field 15 degrees in elevation. The affects of this parameter upon the average cumulative probability of detection $\bar{P}_c(R_i)$ are shown in the following figures for the case of a Cessna 180 in several geometries. In all instances the Cessna 180 has a speed of 80 knots and the observer aircraft has a speed of 240 knots (K = 3).

Figure 22 – Average Cumulative Probability of Detection versus Time Until Impact, Cessna 180· bearing 0°, closing velocity 540 ft/sec, visibility 15 miles, aspect 0°, effective range 1 nautical mile.

Figure 23 – Average Cumulative Probability of Detection versus Time Until Impact, Cessna 180: bearing 0°, closing velocity 540 ft/sec, visibility 15 miles, aspect 0°, effective range 2 nautical miles.

Figure 24 – Average Cumulative Probability of Detection versus Time Until Impact, Cessna 180 bearing 0°, closing velocity 540 ft/sec, visibility 15 miles, aspect 0°, effective range 3 nautical miles.

Figure 25 – Average Cumulative Probability of Detection versus Time Until Impact, Cessna 180: bearing 16.7°, closing velocity 321 ft/sec, visibility 15 miles, aspect 120°, effective range 2 nautical miles.

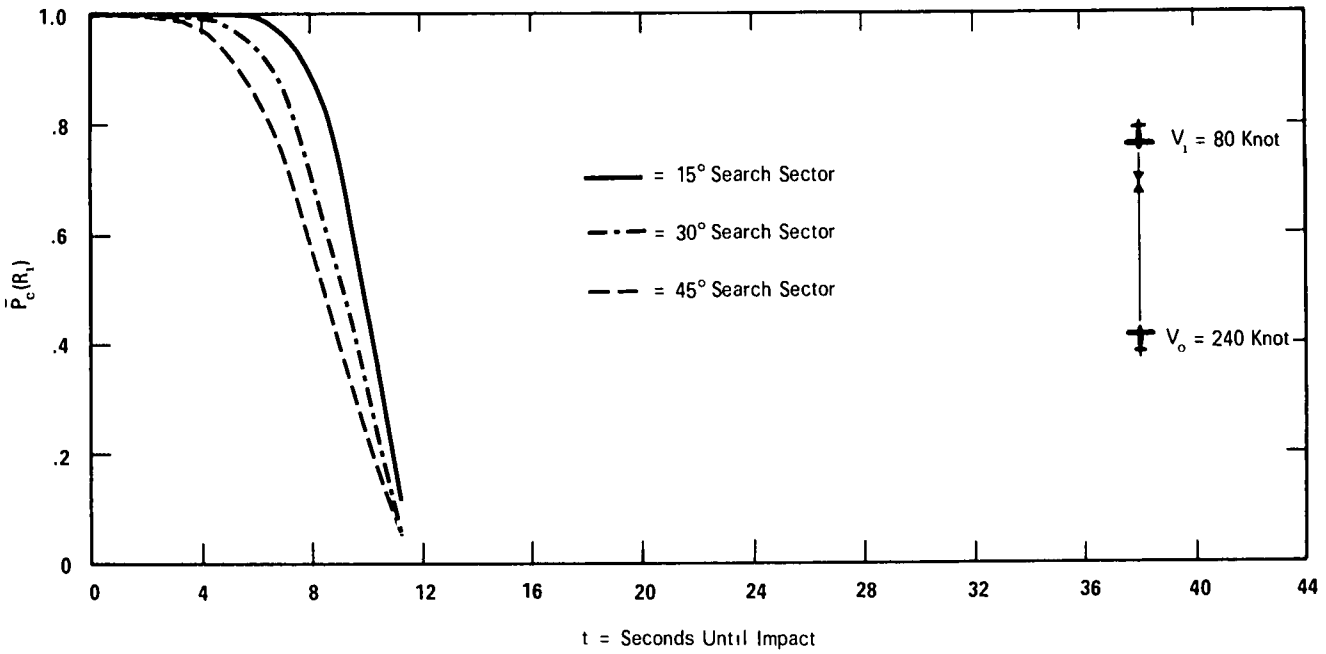

Figure 22. Average Cumulative Probability of Detection Versus Time Until Impact, Cessna 180 bearing 0°, closing velocity 540 ft/sec, visibility 15 miles, aspect 0°, effective range 1 nautical mile.

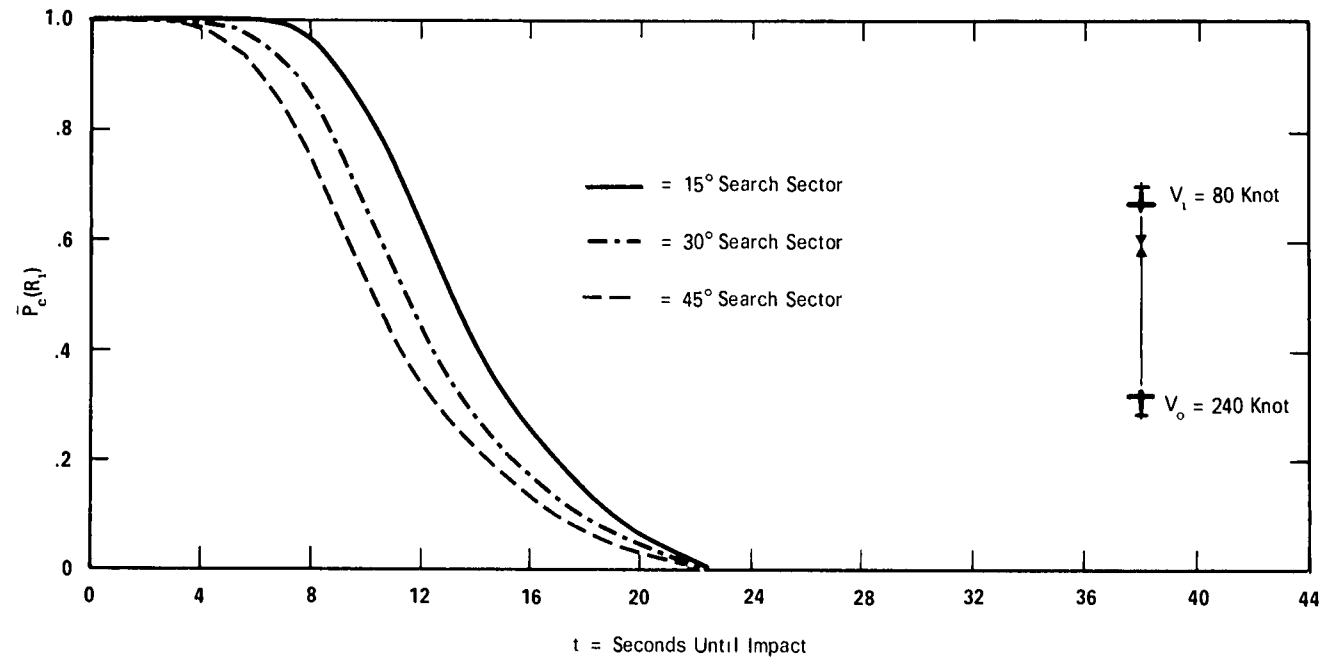

Figure 23. Average Cumulative Probability of Detection Versus Time Until Impact, Cessna 180 bearing 0°, closing velocity 540 ft/sec, visibility 15 miles, aspect 0°, effective range 2 nautical miles.

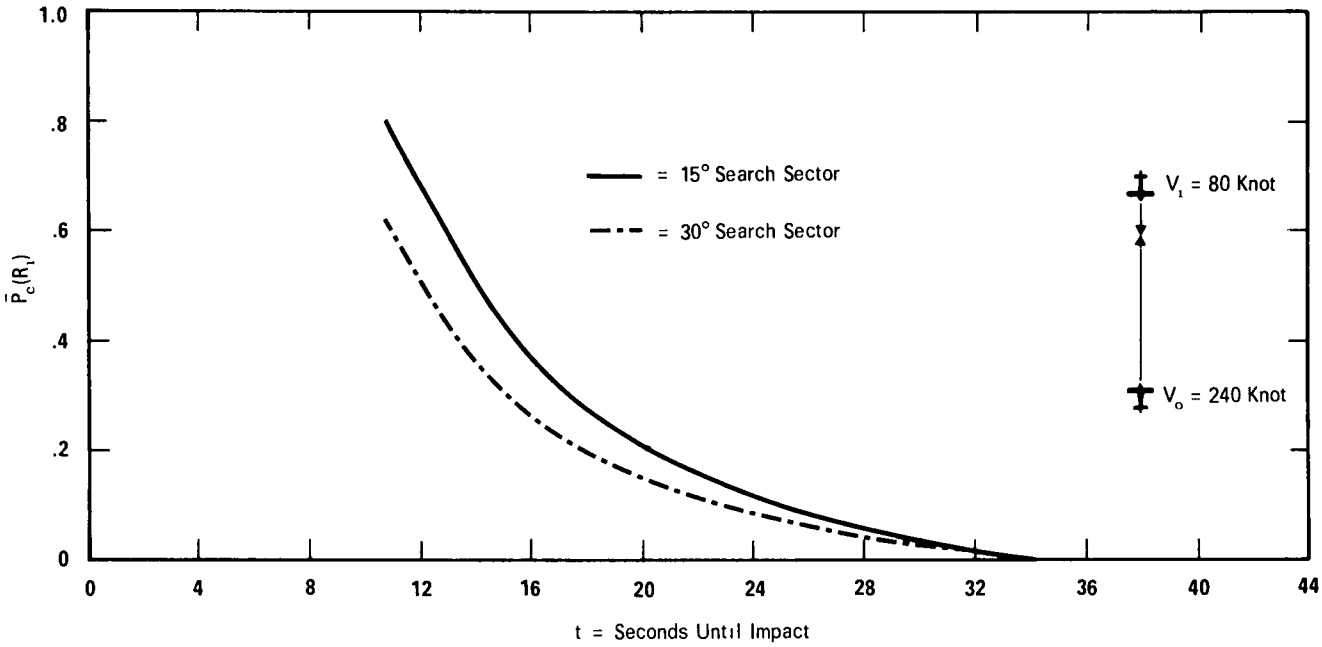

Figure 24. Average Cumulative Probability of Detection Versus Time Until Impact, Cessna 180· bearing 0°, closing velocity 540 ft/sec, visibility 15 miles, aspect 0°, effective range 3 nautical miles.

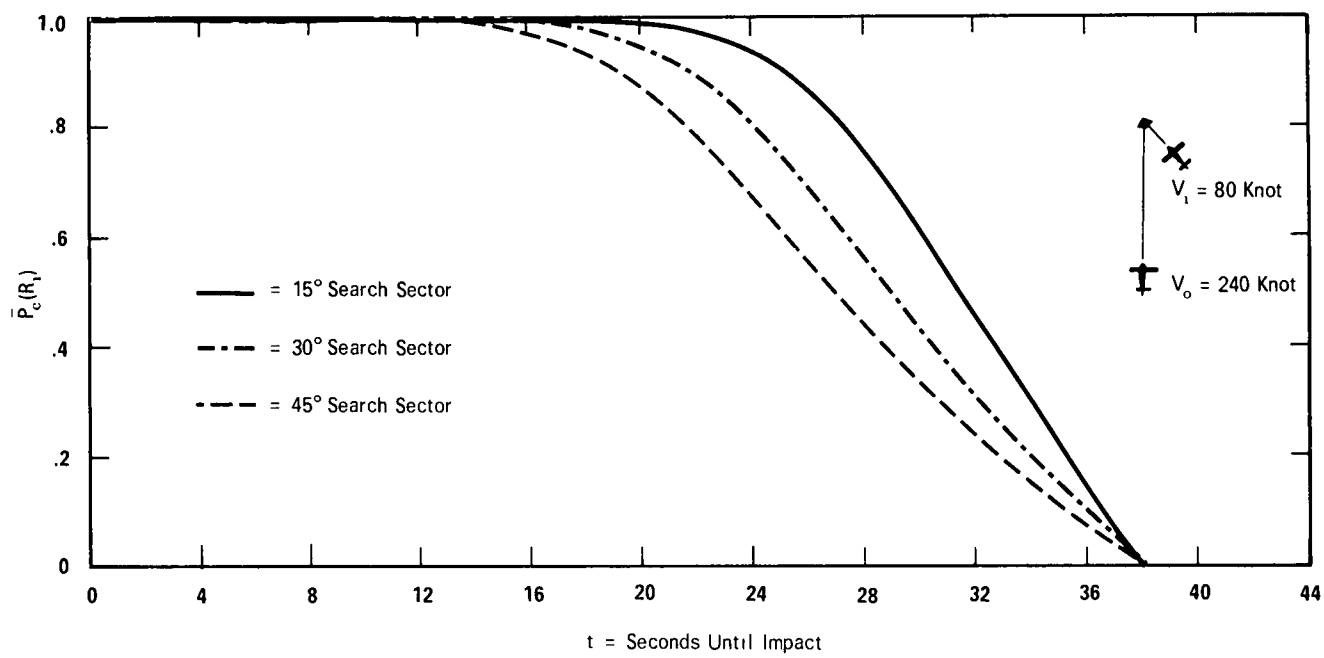

Figure 25. Average Cumulative Probability of Detection Versus Time Until Impact, Cessna 180 bearing 16.7°, closing velocity 321 ft/sec, visibility 15 miles, aspect 120°, effective range 2 nautical miles.

Figure 26 – Average Cumulative Probability of Detection versus Time Until Impact, Cessna 180: bearing 6.5°, closing velocity 275 ft/sec, visibility 15 miles, aspect 160°, effective range 2 nautical miles.

Figure 27 – Average Cumulative Probability of Detection versus Time Until Impact, Cessna 180: bearing 6.5°, closing velocity 275 ft/sec, visibility 15 miles, aspect 160°, effective range 2 nautical miles.

Figure 28 – Average Cumulative Probability of Detection versus Time Until Impact, Cessna 180: bearing 6.5°, closing velocity 275 ft/sec, visibility 5 miles, aspect 160°, effective range 1 nautical mile.

Maximum visual performance would be achieved if the observer could always utilize foveal vision and entirely eliminate the search problem. Figures 22 through 28 verify the obvious fact that the smaller the search sector the higher the average cumulative probability of detection.

As in the case of selecting effective range R_{max} there are many subjective criteria that could be applied to selecting the angular resolution. Many of these would be trade-offs between cost and performance. This study suggests an angular resolution of 30 degrees.

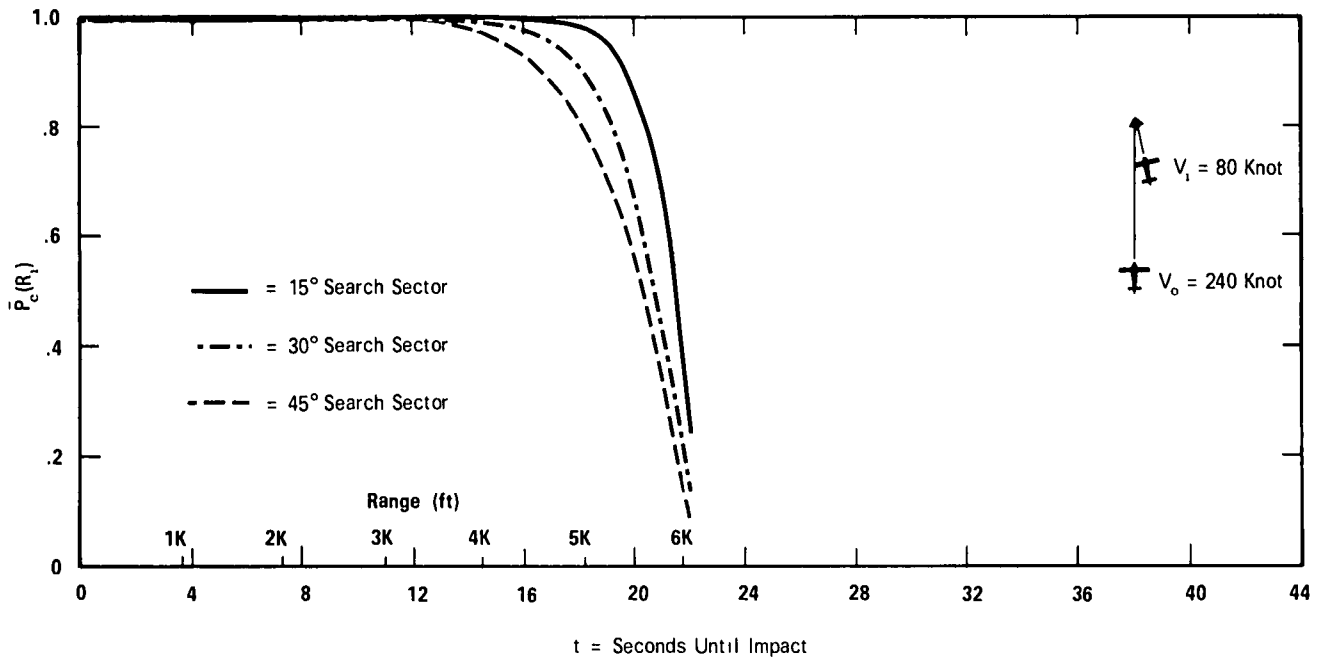

Figure 26. Average Cumulative Probability of Detection Versus Time Until Impact, Cessna 180: bearing 6.5°, closing velocity 275 ft/sec, visibility 15 miles, aspect 160°, effective range 1 nautical mile.

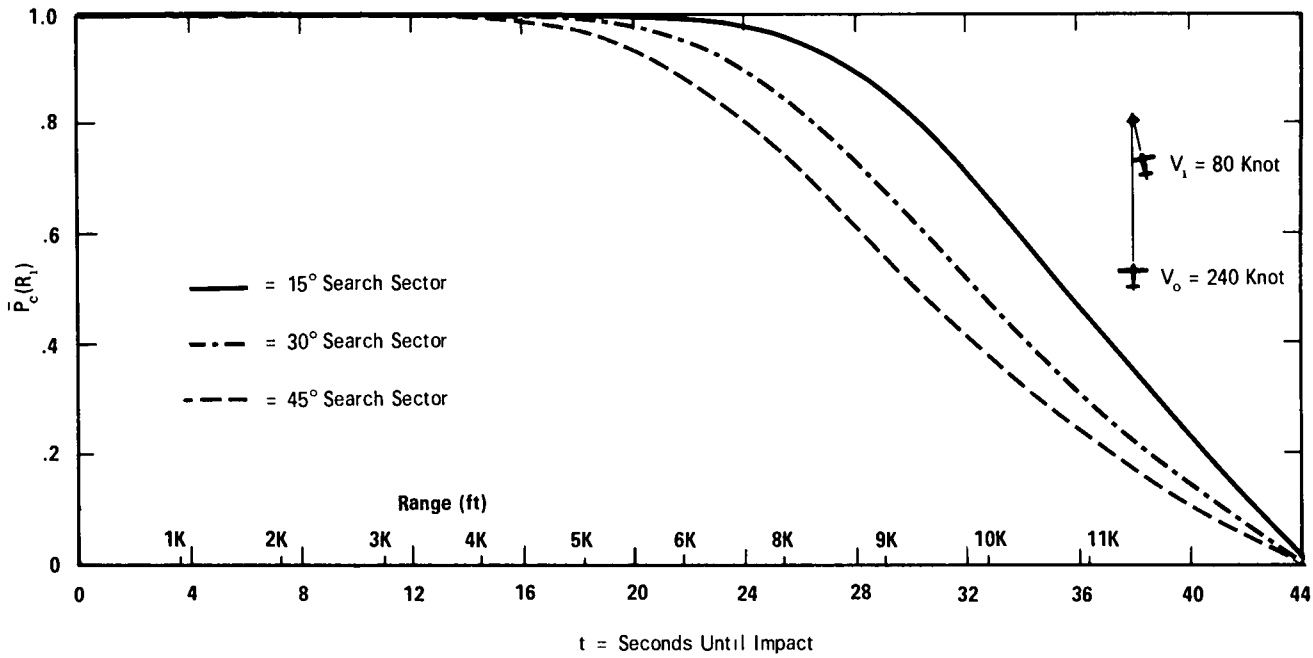

Figure 27. Average Cumulative Probability of Detection Versus Time Until Impact, Cessna 180 bearing 6.5°, closing velocity 275 ft/sec, visibility 15 miles, aspect 160°, effective range 2 nautical miles.

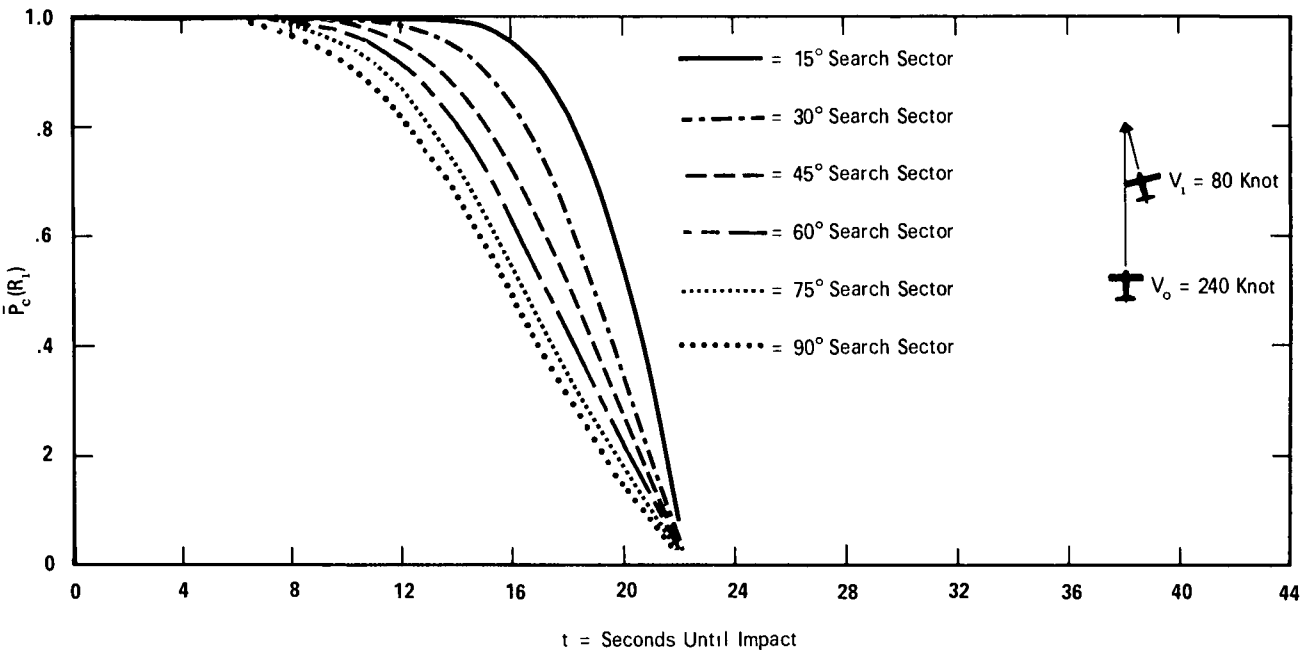

Figure 28. Average Cumulative Probability of Detection Versus Time Until Impact, Cessna 180: bearing 6.5°, closing velocity 275 ft/sec, visibility 5 miles, aspect 160°, effective range 1 nautical mile.

6. SUMMARY AND CONCLUSIONS

It has been shown here that the visual performance of a crew member in a detection task can be significantly improved if he knows when and where to look. It has also been indicated that the concept of a PWI system is a valid approach to supplying the when and where information.

Of the many PWI specifications which influence observer performance, the two most prominent were selected for study: effective range and angular resolution. The quantitative effects of these two specifications have been demonstrated for the case of a Cessna 180 in a number of collision geometries. A study of the results is suggestive that the PWI have an effective range of 2 nautical miles and a resolution of 30 degrees.

Again it should be stressed that this study was limited in scope. Of the hundreds of aircraft types currently flying, only two of the more common were initially examined. Later in the study, finding the smaller Cessna 180 gave a more critical angular subtense, all effort was focused on that one aircraft alone and on the unique contrast map it presented with the one sun location. The effects upon the calculations of different paint schemes and other sun locations should be investigated. Other types of aircraft and other geometries should also be included.

Techniques for the quantitative evaluation of the probability of visually acquiring an aircraft posing a collision threat have been developed by the Visibility Laboratory under funding from the NASA-Ames Research Center. It is believed that these techniques constitute an important tool which can be used to increase the level of understanding of the visual aspects of air collision. It is hoped that this potential will be fully exploited.

UNCLASSIFIED
Security Classification

DOCUMENT CONTROL DATA - R&D

(Security classification of title, body of abstract and indexing annotation must be entered when the overall report is classified)

1 ORIGINATING ACTIVITY *(Corporate author)*

Visibility Laboratory
University of California
San Diego, California 92152

2a. REPORT SECURITY CLASSIFICATION

UNCLASSIFIED

2b. GROUP

3 REPORT TITLE

VISUAL ASPECTS OF AIR COLLISION AVOIDANCE:
COMPUTER STUDIES ON PILOT WARNING INDICATOR SPECIFICATIONS

4 DESCRIPTIVE NOTES *(Type of report and inclusive dates)*

Final Report

5 AUTHOR(S) *(Last name, first name, initial)*

Edwards, Gerald D. and Harris, James L., Sr.

6 REPORT DATE	7a. TOTAL NO OF PAGES	7b NO OF REFS
February 1972	25	3

8a CONTRACT OR GRANT NO	9a ORIGINATOR'S REPORT NUMBER(S)
NGR-05-009-059	SIO Ref. 72-3
b.	
c.	9b OTHER REPORT NO(S) *(Any other numbers that may be assigned this report)*
d.	

10 AVAILABILITY LIMITATION NOTICES

Distribution of this Document is Unlimited

11 SUPPLEMENTARY NOTES	12 SPONSORING MILITARY ACTIVITY
	NASA-Ames Research Center Moffett Field, California 94306

13 ABSTRACT

This report describes techniques of computer calculations used to analyze the potential for improving visual acquisition of collision threats by means of Pilot Warning Indicator systems (PWI). It is a parametric study giving the quantitative effects of PWI resolution and effective range upon the average cumulative probability of detection.

DD FORM 1 JAN 64 1473

UNCLASSIFIED
Security Classification

14 KEY WORDS	LINK A		LINK B		LINK C	
	ROLE	WT	ROLE		ROLE	WT
Pilot warning indicator effective range						
Pilot warning indicator angular resolution						
Human visual detection capabilities and limitations						
Probability of visual detection						